Brain working memory network indices as landmarks of intelligence

Mohammadreza Khodaei[a], **Paul J. Laurienti**[a,b], **Dale Dagenbach**[c], **Sean L. Simpson**[a,d,*]

[a]Virginia Tech-Wake Forest University School of Biomedical Engineering and Sciences, Wake Forest University School of Medicine, Winston-Salem, NC, USA

[b]Department of Radiology, Wake Forest University School of Medicine, Winston-Salem, NC, USA

[c]Department of Psychology, Wake Forest University, Winston-Salem, NC, USA

[d]Department of Biostatistics and Data Science, Wake Forest University School of Medicine, Winston-Salem, NC, USA

Abstract

Identifying the neural correlates of intelligence has long been a goal in neuroscience. Recently, the field of network neuroscience has attracted researchers' attention as a means for answering this question. In network neuroscience, the brain is considered as an integrated system whose systematic properties provide profound insights into health and behavioral outcomes. However, most network studies of intelligence have used univariate methods to investigate topological network measures, with their focus limited to a few measures. Furthermore, most studies have focused on resting state networks despite the fact that brain activation during working memory tasks has been linked to intelligence. Finally, the literature is still missing an investigation of the association between network assortativity and intelligence. To address these issues, here we employ a recently developed mixed-modeling framework for analyzing multi-task brain networks to elucidate the most critical working memory task network topological properties corresponding to individuals' intelligence differences. We used a data set of 379 subjects (22–35 y/o) from the Human Connectome Project (HCP). Each subject's data included composite intelligence scores, and fMRI during resting state and a 2-back working memory task. Following comprehensive quality control and preprocessing of the minimally preprocessed fMRI data, we extracted a set of the main topological network features, including global efficiency, degree, leverage centrality, modularity, and clustering coefficient. The estimated network features and subject's confounders were then incorporated into the multi-task mixed-modeling framework to investigate how brain network changes between working memory and resting state relate to intelligence score. Our results indicate that the general intelligence score (cognitive composite score) is

associated with a change in the relationship between connection strength and multiple network topological properties, including global efficiency, leverage centrality, and degree difference during working memory as it is compared to resting state. More specifically, we observed a higher increase in the positive association between global efficiency and connection strength for the high intelligence group when they switch from resting state to working memory. The strong connections might form superhighways for a more efficient global flow of information through the brain network. Furthermore, we found an increase in the negative association between degree difference and leverage centrality with connection strength during working memory tasks for the high intelligence group. These indicate higher network resilience and assortativity along with higher circuit-specific information flow during working memory for those with a higher intelligence score. Although the exact neurobiological implications of our results are speculative at this point, our results provide evidence for the significant association of intelligence with hallmark properties of brain networks during working memory.

Keywords

Intelligence; Brain network; Working memory; Resting state; fMRI; Fluid and crystalized intelligence; Global efficiency; Degree difference; Leverage centrality; General intelligence

1. Introduction

Understanding the neural basis of intelligence has been a longstanding research focus for neuroscientists, as intelligence can significantly impact an individual's academic achievement (Laidra et al., 2007; Malykh, 2017). Furthermore, studies have reported that a low intelligence score is associated with autism (Crespi, 2016) and is a risk factor for developing dementia and Alzheimer's disease (Yeo et al., 2011; Anderson et al., 2020) and amyotrophic lateral sclerosis (ALS) (Longinetti et al., 2017) in later life. Intelligence has also been related to other conditions, including stroke, coronary heart disease (Kajantie et al., 2012), obesity (Kanazawa, 2013), and some types of cancer (Kanazawa, 2014). Recent neuroimaging techniques, including functional magnetic resonance imaging (fMRI), diffusion tensor imaging (DTI), and structural MRI morphometry, have provided unique insight into the study of the brain and intelligence (Satary Dizaji et al., 2021), which has resulted in several theories about their relationship (Barbey, 2018).

2. Intelligence theories based on neuroimaging findings

Most early theories of brain and intelligence focused on activation-based analysis. The neural efficiency hypothesis of intelligence is one of the first neuroimaging extracted theories of intelligence, stating that individuals with higher intelligence scores demonstrate lower brain activation during cognitive tasks (Haier et al., 1988). This theory was later disputed in a review stating that while early task-based studies align with this hypothesis, recent studies have cast doubt on this hypothesis or have identified that some variables like gender, task type, and task complexity can affect this relationship (Neubauer and Fink, 2009). The early theories were also focused on localizing the brain area related to intelligence, including the Lateral Prefrontal Cortex (PFC) theory, stating that the individual

differences in general intelligence are related to functionally localized regions in the lateral prefrontal cortex (Duncan and Owen, 2000). The network theories of intelligence emerged with the Parieto-Frontal Integration Theory (P-FIT). In a review study of neuroimaging studies (i.e., fMRI, DTI, positron emission tomography (PET), and magnetic resonance spectroscopy (MRS)) of intelligence, Jung and Haier reported that variation in the frontal and parietal regions and connections of the brain predict individual differences in intelligence. They described their finding as P-FIT (Jung and Haier, 2007). However, the inferred networks related to intelligence were obtained mainly by activation-based analysis, necessitating the direct investigation of brain networks (Yoo et al., 2019) and intelligence.

3. Network investigation of intelligence and the brain

With the emergence of network neuroscience, the direct study of the brain network as an integrated system has grabbed attention. The ability of network science to tackle the complex problem of investigating interactions between brain regions has made it a valuable tool for functional brain analysis (Bassett and Sporns, 2017). The current literature has promoted several network topological characteristics as the critical features of individuals with higher intelligence scores, including global efficiency, modularity, centrality measures, and clustering coefficient. Global efficiency, the inverse of average shortest paths (Bassett and Bullmore, 2006) of the brain network, has been associated with intelligence in resting state fMRI (van den Heuvel et al., 2009; Pamplona et al., 2015), electroencephalogram (EEG) (Langer et al., 2012), and DTI (Li et al., 2009; Zalesky et al., 2011; Yeo et al., 2016) studies. Van den Heuvel et al. suggested that the shorter functional path length between brain regions helps with more efficient information integration in individuals with higher intelligence scores (van den Heuvel et al., 2009). In contrast, a few studies report no association between global efficiency and general intelligence (Kruschwitz et al., 2018; Hilger et al., 2017a). Neuroimaging studies of intelligence have also investigated measures of network centrality (Langer et al., 2012; Hilger et al., 2017a, 2017b). Centrality measures help identify the network's hubs, assortativity, and resilience. Most of these studies have focused on investigating the hubs. For example, using functional connectivity extracted from EEG data, the parietal lobe was identified as the central hub of the brain related to intelligence based on the high correlation between its degree centrality and intelligence (Langer et al., 2012). Intelligence has also been related to measures of modularity (Hilger et al., 2017a, 2020). Modularity characterizes how well a network subdivides into subnetworks for an efficient information process. High modularity represents high within subnetwork connections and low between subnetwork connections (Newman, 2006). Hilger et al. reported that while no association between intelligence and global modularity features was observed, node-specific measures (within module degree and participation coefficient) were associated with intelligence (Hilger et al., 2017a). Finally, intelligence has been linked with the clustering coefficient (van den Heuvel et al., 2009; Pamplona et al., 2015; Langer et al., 2012). The clustering coefficient is another measure of the segregation of the network. Segregation defines a network's ability to perform specific tasks in highly intraconnected subnetworks. The existing brain network studies of intelligence highlight links between topological features and differences in an individual's intelligence. However, the literature still lacks a comprehensive study of all these network measures in a multivariate framework.

4. Working memory and measures of intelligence

Neuroimaging studies of intelligence have focused on three main intelligence measures: fluid, crystallized, and general intelligence. Cattell proposed the idea of fluid and crystallized intelligence (Cattell, 1987). Fluid intelligence is an individual's ability to solve new problems without prior knowledge. Cattell referred to this ability as fluid intelligence as it "has the 'fluid' quality of being directable to almost any problem." On the contrary, crystallized intelligence is an individual's gained knowledge and experience and is associated with language, verbal skills, and academic success. He referred to gained knowledge as crystallized intelligence as it "is invested in the particular areas of crystallized skills which can be upset individually without affecting the others" (Cattell, 1987). Fluid and crystallized intelligence each can capture a specific part of the general cognitive ability, known as general intelligence. Spearman proposed the idea of general intelligence in the early 19th century after observing that an individual's success rate in different cognitive tasks positively correlates with this measure. He defined this overlap of success rate in the different cognitive tasks as general intelligence (Duncan et al., 2000). In this study, we will investigate all three measures of intelligence and their relationship to functional brain network architecture during a working memory task, during resting state, as well as the difference in network topology between the working memory and resting state.

Working memory is a process that transiently maintains and manipulates information in a highly accessible state (Cowan, 2014). Prior studies have shown that working memory has a close relationship with fluid (Kane et al., 2005) and general intelligence (Colom et al., 2004) and also can affect crystallized intelligence (Alloway and Alloway, 2009). In fact, it has been one of the most common tasks used in fMRI studies of intelligence to find brain regions and networks related to intelligence (Tang et al., 2010; Waiter et al., 2009; Finn et al., 2015; Assem et al., 2020; Cole et al., 2012; Basten et al., 2013). However, network neuroimaging studies of intelligence have mainly focused on resting state network characteristics. The literature still lacks a comprehensive investigation of the relationship between brain topological network features and intelligence during a working memory task.

Taken together, previous studies highlighting links between intelligence and brain network properties demonstrate the network fingerprint of intelligence. However, most of these studies have focused on the resting state network, with the majority of the working memory studies focusing on activation instead of network analyses. Furthermore, these studies mostly focused on one or two graph measures, such as modularity, which may have low sensitivity and specificity, or mass-univariate vertex or edge comparisons that neglect the network's multivariate topological properties. More specifically, most studies compared the mean of nodal topological network measures across subjects which fails to capture the variability at the nodal level. Finally, there is a lack of studies investigating brain assortativity and how it relates to intelligence. Assortativity relates to tendency of nodes in a network to connect to other nodes with the same specific characteristic. To address these issues, we used our recently developed multivariate mixed modeling framework (Simpson et al., 2019; Simpson and Laurienti, 2015) for multi-task data to study the association between intelligence composite scores and brain network topological properties during a working memory task as it compared to resting state. This model can evaluate the relationship

between multiple variables of interest, and topological network features on the whole brain network structure, which enables characterizing the most critical network measures during brain working memory compared to the resting state for intelligent individuals.

5. Material and methods

5.1. Data acquisition

We used a subset from 1200 human connectome project young adult (HCP-YA) data (Van Essen et al., 2013) with resting state, task-based fMRI during a working memory task, and NIH cognitive scores available for each subject. Resting state fMRI data acquisition was done in two runs with different phase encoding (RL and LR) using a 3T Siemens connectome-Skyra scanner with TR = 720 ms, voxel size = $2 \times 2 \times 2$ mm and scan time of 864 s/run (1200 vol/run). Task-based fMRI data acquisition was performed with the same imaging protocol (two runs) but in shorter time (303 s/run (420 vol/run)). Each task-based run included eight blocks (four 0-back and four 2-back), with each block lasting for 25 s. Four categories of pictures, including faces, tools, places and body parts, were used as stimuli, with each run including two blocks of each image type. At the start of each block, a 2.5 s cue was presented to specify the task type and the cue (Barch et al., 2013a).

Cognitive abilities scores were obtained using NIH cognitive toolbox tests (http://www.nihtoolbox.org). The fluid intelligence composite score was assessed by five tests, including two executive function tests (inhibition and cognitive flexibility), a processing speed test, a working memory test, and an episodic memory test. Crystalized intelligence composite score was estimated by two verbal tasks, including language reading decoding and vocabulary comprehension. The cognitive function composite score, general intelligence, was estimated by averaging the normalized scores of fluid and crystalized cognitive measures, followed by scaling scores based on the new distribution (Heaton et al., 2014; Barch et al., 2013b). Fig. 1 illustrates the cognitive tests used to assess each cognitive ability and the structure of the composite scores. This study investigated crystallized, fluid, and general intelligence composite scores' relationship with brain network differences during a working memory task as compared resting state.

5.2. Preprocessing

We used the minimally preprocessed resting state and working memory task fMRI data provided by the HCP (Glasser et al., 2013). Out of 1200, 937 subjects had both resting state

and working memory task data in our version of HCP data. Prior to any preprocessing, data went through a quality control check, and subjects with high motion and distortion were removed from the study. More specifically, 116 subjects had artifact issues (74 subjects had movement greater than 2 mm or rotation higher than 2°, 32 subjects had warping issues and 25 still had fMRI signal artifacts after AROMA noise correction). In addition, we excluded subjects with family relations by finding subjects with the same family identification number and selecting an individual randomly. Out of 937, there were 435 subjects with unique family IDs. Finally, we removed subjects with cognitive test incompletion and missing demographic information. These procedures yielded a final sample size of 379 subjects. We further divided the data into two high and low scoring groups based on the median of three measures of intelligence (general, fluid, and crystallized).

To further clean the data, we removed the first 10 s of the data (14 vol). Next, we performed motion correction using ICA-Aroma (Pruim et al., 2015) to remove any motion artifacts. Bandpass filtering was done with 0.009 and 0.08 cut off to remove the scanner's low-frequency drift and physiological low and high-frequency noises. Next, we concatenated the two runs (RL and LR phase encoding). We performed a single regression analysis using SPM12 to remove unwanted signals from time series data. Regressors included the whole brain mean signals for gray matter, white matter and cerebrospinal fluid (CSF), realignment parameters, and a final regressor for the concatenation of the two runs. For working memory data we included additional regressors extracted by modeling the block design for 0-back, rest, and cue blocks. For both rest and task data, we removed artificial excess high-frequency noise derived from the concatenation of the runs, using a continuous wavelet transform with a window size of 30 s, centered at the joint of the two runs.

HCP's working memory task data includes working memory blocks (2-back blocks), long-term memory blocks (0-back blocks), and the resting state. This design is a preferable design for activation-based analysis. However, using the whole working memory task time series data in a correlation based analysis to study working memory can be misleading. We extracted the time series related to only the 2-back task and concatenated them (Fig. 2) to investigate the brain oscillation associated with the working memory instead of the whole series of events.

Following the preprocessing, we parcellated the brain into 268 regions using the Shen Atlas (Shen et al., 2013) and computed the mean time series of voxels in each region for each participant. Connectivity matrices were estimated by computing the correlation between average signals of all region pairs. Two versions of the correlation matrices were estimated, positive weighted connectivity and positive binary connectivity keeping all positive edges regardless of strength. Five network topology measures that cover the main categories of systemic network properties from the positive connectivity matrix were extracted. Fig. 3 illustrates the data preparation steps.

5.3. Multitask mixed modeling framework

We used the two-step mixed modeling framework for multi-task data to analyze functional brain networks during working memory compared to the resting state (Simpson et al., 2019; Simpson and Laurienti, 2015). This model assesses both probabilities of a connection

(present/absence) and the strength of a connection based on the covariate of interest, network systemic characteristics (topological network measures), subjects' biological variables (e.g., age, sex, handedness), the tasks and the interactions. Unlike the common methods that perform a univariate comparison of metrics across tasks, this model considers the association between population network differences and individuals' variability in network differences across tasks and covariate of interests such as cognitive scores and health outcomes. Two equations govern the multi-task mixed modeling framework:

$$\text{logit}(p_{ijkl}\backslash(\beta_{rl}; b_{rli})) = X'_{ijkl}\beta_{rl} + Z'_{ijkl}b_{rli} \tag{1}$$

$$\text{FTZ}(S_{ijkl}(\beta_{sl}; b_{sli})) = X'_{ijkl}\beta_{sl} + Z'_{ijkl}b_{sli} + e_{ijkl} \tag{2}$$

The first equation models the probability of the existence of connections (p_{ijkl}) using a logistic mixed model, and the second equation models the Fisher's Z-transform of the strength of the connections (S_{ijkl}). β_{rl} and β_{sl} denote vectors related to population parameters (fixed effects). These betas relate the probability and strength of the connection between node j and node k for subject i using a set of covariates (X_{ijkl}) for the lth task. b_{rli} and b_{sli} are vectors of the subject (i) and node-specific parameters (random effects). These b values estimate the extent to which the subject and node (Z'_{ijkl}) vary about the population average (β_{rl}, β_{sl}) for the lth task. See Simpson et al. (Simpson et al., 2019; Simpson and Laurienti, 2015) for further description regarding the mixed modeling framework for multi-task data; Fig. 4 shows a schematic of the used mixed model framework.

We included five measures of brain network topology, including average global efficiency, average leverage centrality (Joyce et al., 2010), average clustering coefficient, degree difference, and modularity (using Newman's spectral community detection method) to cover the main categories of systemic network properties. The rational for using the average, and in the case of degree, the difference, of topological measures is that the designed mixed modeling framework models the edge strength and probability based on topological network characteristics that are node specific. To expand the node specific characteristic to edges, the average (in the case of degree the difference) of the two nodes topological characteristic for each edge is computed. In addition, we added Euclidean spatial distance between brain regions to the model. Fig. 5 illustrates the mixed modeling framework (top) and edge topological network measures (bottom) for a hypothetical brain network. We used the WFU_MMNET toolbox (Bahrami et al., 2019) for the estimation of Pearson's correlation networks, topological network measures, and spatial distances.

The covariate of interest in this study was the IQ groups (high and low intelligence score) based on each of three composite cognitive scores (fluid, crystallized, and general intelligence). We incorporated a working memory task regressor as a task identifier (resting state vs. working memory) in the model. Gender (categorical), age (continuous), handedness (continuous, – 100   x   100), BMI (continuous), total household income with eight levels (continuous), education level (categorical with three levels, level 1 (11 years of education completed), level 2 (12–16), and level 3 (17)), race (categorical with six categories – type 1

(Am. Indian/Alaskan Nat.), type 2 (Asian/Nat.Hawaiian/Other Pacific Is.), type 3 (Black or African Am.), type 4 (White), type 5 (More than one), type 6 (Unknown or Not Reported)), ethnicity (categorical with three categories – type 1 (Hispanic/Latino), type 2 (Not Hispanic/ Latino), type 3 (Unknown or Not Reported)), DSM4 alcohol abuse, demonstrates whether participant met DSM4 criteria for alcohol abuse (categorical), DSM4 alcohol dependence, indicates whether participant met DSM4 criteria for alcohol dependence (categorical), and smoking status (categorical) were included as biological regressors (X_i). The five topological edge features, covariate of interest, task identifier, biological demographic information, and interactions were all incorporated into the mixed modeling framework. Mixed model analyses were run using SAS code from our previous work (Simpson et al., 2019).

6. Results

We removed subjects with low image quality, high motion during imaging, missing data, and family relations through our quality control check. This yielded 379 subjects. The sample's demographic information and NIH toolbox cognitive scores are listed in Table 1.

7. Mixed model framework results

The parameter estimates show the association between topological network measures and network connections during the working memory task (compared to resting state) for the high scoring group compared to the low scoring group based on their intelligence. Fig. 6 illustrates the breakdown of the parameter of interest.

We performed separate analyses for fluid, crystallized, and general intelligence. The summary of results is presented in Tables 2–4, with the significant results in bold format. The $\beta_{s, WM \times IQ \times Eglob\_avg}$, $\beta_{s, WM \times IQ \times lev\_avg}$ and, $\beta_{s, WM \times IQ \times deg\_diff}$ show the parameter estimates for average global efficiency, leverage centrality, and degree difference, respectively. The strength model analysis demonstrated higher increase in association between network topological measures and strength of the connections for the high general intelligence group (Table 2). In summary, our results showed that compared to the resting state, during the working memory task the high intelligence group had:

- Stronger positive association between global efficiency and the strength of the network's connections ($\beta = 0.2325$, FDR $= 0.0236$). More specifically, in the individuals with higher intelligence scores, with an increase in the global efficiency of nodes, the connected edges become stronger.

- Stronger negative association between connectivity strength and the two network centrality measures, including degree difference ($\beta = 0.2325$, FDR $= 0.0267$) and leverage centrality ($\beta = -0.00771$, FDR $= 0.0328$). As these measures increase for an edge, the individuals with higher intelligence form weaker connections for those edges.

Fig. 7 illustrates the significant effects of intelligence on the relationships between connection strength and network features, including global efficiency, degree difference, and leverage centrality during working memory task compared to the resting state for high and low scoring general intelligence groups. The increase in the positive slope demonstrates

that when higher intelligence individuals switch from resting state to working memory, the association between global efficiency and connection strength of their brain network increases more as compared to the lower intelligence group (Fig. 7a). More specifically, edges with higher average global efficiency will have higher strength connections. In contrast, there is a decrease in the negative slope between connection strength and degree difference and leverage centrality for those in the higher intelligence group (Fig. 7b and Fig. 7c). Therefore, an edge with a high degree difference and high average leverage centrality will have weaker connections.

The analysis of the binary model for general intelligence did not yield any significant results; there was no evidence that general intelligence changes the relationship between the probability of a connection existing and network measures during working memory as compared to resting state (Table 2). We further investigated the effect of fluid and crystalized cognitive scores on topological network measures. While not as significant as general intelligence, fluid intelligence marginally affects the degree difference (FDR = 0.057) relationship with network strength during working memory tasks relative to resting state. Our findings also demonstrate a positive influence of crystalized intelligence on the relationship between global efficiency and the strength of the connections (FDR = 0.0269). The binary model analysis again did not show significant differences between high and low intelligence scoring groups. Tables 3 and 4 exhibit the modeling results for fluid and crystallized intelligence, respectively. The full table of the parameter estimates for the two-part mixed model analysis for each measure of intelligence can be found in Tables 1–6 of the Supplementary Material.

We conducted two additional analyses to explore the data. In the first analysis, we attempted to run the model with intelligence as a continuous variable, but it failed to converge. In the second analysis, we trimmed the resting state time series to match the length of the working memory data. This adjustment accounts for the bias resulting from the working memory and resting state time series having different lengths, but it comes with the cost of introducing more noise into the resting state time series. In line with our previous findings, we observed a significant association between global efficiency and crystallized intelligence. However, while the other parameter estimates showed the same sign and comparable magnitude as in the previous analysis, the estimates were not significant due to inflated error terms. The results of this analysis are presented in Table 7 of the Supplementary Material.

8. Discussion

8.1. Summary

The present study sought to identify the changes in brain topological network properties associated with intelligence when the brain switches from a resting state to a working memory task. This goal was achieved using the recently developed mixed modeling framework for analyzing multi-task brain networks. Similar to activation-based analysis in which brain activation during a task is compared to the resting state, this framework enables studying brain network changes during a task compared to the resting state. More specifically, here, we investigated the changes in the relationship between topological network features and connection characteristics (strength and probability of existence)

related to a biological outcome (intelligence) during brain working memory as compared to resting state. To our knowledge, this is the first study investigating intelligence association with topological network features during working memory compared to the resting state. Here we report global efficiency, degree difference, and leverage centrality as the main network features related to intelligence during brain working memory tasks as compared to the resting state.

8.2. Intelligence test

One of the main issues with neuroimaging studies of intelligence is the diversity among the intelligence tests used, which makes cross study comparisons complicated. In the neuroimaging literature, fluid intelligence has been assessed by single measures such as the Raven Progressive Matrix Test (Langer et al., 2012; Kruschwitz et al., 2018; Waiter et al., 2009; Finn et al., 2015; Cole et al., 2012; Basten et al., 2013; Cohen and D'Esposito, 2016; Dizaji et al., 2019) and Kaufman Brief Intelligence Test (Assem et al., 2020). It has also been estimated using composite measures such as NIH composite fluid intelligence score (Kruschwitz et al., 2018; Finn et al., 2015) and different versions of the Wechsler performance IQ test (van den Heuvel et al., 2009; Pamplona et al., 2015; Hilger et al., 2017b; Tang et al., 2010). NIH composite score (Kruschwitz et al., 2018; Finn et al., 2015) and the Wechsler full scale IQ (van den Heuvel et al., 2009; Pamplona et al., 2015; Hilger et al., 2017a; Hilger et al., 2017b; Hilger et al., 2020; Tang et al., 2010; Fischer et al., 2014) were also the main tests used for crystalized and general intelligence. Even though correlations among different intelligence tests have been reported, the inconsistency among the intelligence tests used makes the comparison of results challenging. Our study used the NIH toolbox scores with all three available intelligence measures (fluid, crystallized, and general intelligence).

8.3. Global efficiency

In recent years, there has been growing debate over whether or not global efficiency is related to intelligence. Global efficiency refers to the inverse average of the shortest path length. By intuition, it comes to mind that there is a shorter path length between brain regions in more efficient brains, which helps with the faster and easier flow of information between different brain regions. Van Den Heuvel et al. were among the first studies to report the positive correlation between global efficiency and intelligence (van den Heuvel et al., 2009). Two other functional studies also emphasized this association (Pamplona et al., 2015; Langer et al., 2012). Furthermore, DTI studies of structural connectivity of intelligence have also confirmed this association (Li et al., 2009; Zalesky et al., 2011; Yeo et al., 2016).

Here we used a different approach for studying the global efficiency association with intelligence. We investigated how intelligence changes the relationship between connection strength and global efficiency during working memory compared to the resting state. Our results demonstrated that the group with higher intelligence scores has a stronger positive relation between global efficiency and connection strength during working memory compared to resting state. The positive relationship implies that edges with higher global efficiency have stronger connections. These strong connections, connecting two nodes with short paths to all other nodes, might act as superhighways for the global flow of information

during working memory tasks. Although indirectly, our result aligns with the previous report on the association between intelligence and global efficiency. In contrast, two recent functional network studies, including a study on HCP data, did not yield any association between intelligence and functional connectivity during resting state (Kruschwitz et al., 2018; Hilger et al., 2017a). We used the same database (HCP) as in the Kruschwitz et al., 2018 study (Kruschwitz et al., 2018); however, we used a different approach. Moreover, our study focused on changes between resting state and working memory, which makes comparing our results with theirs challenging. Our separate analysis of crystallized and fluid intelligence also demonstrated an association between crystallized intelligence and global efficiency, which was previously observed in the Longer et al. EEG study (Langer et al., 2012).

8.4. Degree difference and leverage centrality

We used degree difference and leverage centrality measures to investigate the association of intelligence with assortativity of the brain network. Assortativity refers to the tendency of the network nodes to attach to others with a similar characteristic. This characteristic in functional brain network studies is typically degree. Assortativity has been related to the network's resilience against damage to its nodes (Newman, 2002). In disassortative networks, the highly connected nodes (hubs) are connected to low degree nodes. This network topology makes these networks highly dependent on highly connected nodes, as any dysfunction of these hubs interrupts the information flow. We observed a higher increase in the negative relationship between degree difference and network strength for the high intelligence group. This association indicates that nodes with a high degree difference (low assortativity) have lower connection strength during working memory relative to the resting state in the high intelligence group compared to the low intelligence group. The weaker connections between high degree nodes (hubs) and low degree nodes might lead to more circuit-specific information flow during working memory which helps with a more segregated flow of information in higher intelligent individuals. This circuit-specific information flow is not related to the spatially local flow of information; they indicate local information flow among neighbor nodes in the network.

Leverage centrality characterizes the connectivity of a node relative to its neighbors. More specifically, it investigates the node degree relative to its neighbors' degrees. Unlike global efficiency, leverage centrality does not quantify information flow along the shortest path; instead, it investigates the disparity of node degrees in a small neighborhood that characterize local information flow (Joyce et al., 2010). Our results showed a larger negative association between leverage centrality and connection strength for those with higher intelligence scores when their working memory network was compared to the resting state network. More specifically, nodes with higher leverage centrality had weaker connections when the high intelligence group switched from resting state to working memory. The weaker connections of high leverage centrality edges make the network more locally assortative. This also leads to a more circuit-specific flow of information.

Taken together, these results highlight links between intelligence and the relationship between connection strength and assortativity. Specifically, in the group with higher

intelligence scores, we observed that nodes with higher assortativity had stronger connections during working memory compared to the resting state. Assortativity has been related to resilience (Newman, 2002) and the local information flow of the network (Joyce et al., 2010). In line with our findings, Santarnecchi et al. reported that brighter individuals have a more resilient network against systemic insults during the resting state (Santarnecchi et al., 2015). Furthermore, local information flow measures, like the clustering coefficient (van den Heuvel et al., 2009; Pamplona et al., 2015), have been related to intelligence, however, to our knowledge, our study is the first that investigates local information flow in the context of assortativity.

8.5. Modularity and clustering coefficient

Our results showed no effect of intelligence on the relationship between modularity or clustering coefficient of the brain with existence and strength of the connections when the brain shifts from the resting state to the working memory task. Both measures are associated with information segregation. Modularity captures the level of segregation of subnetworks whereas clustering coefficient captures the interconnectivity of a nodes neighbors. Several studies have focused on the relationship between modularity and intelligence, with diverse findings for global and region-specific modularity (Hilger et al., 2017a, 2020; Santarnecchi et al., 2017). Here we found no modular network changes related to intelligence during brain change from resting state to working memory.

9. Conclusion

In summary, this network based study sheds light on the complex relationship between intelligence and brain functional network during working memory as compared to resting state. More specifically, we explored how intelligence is associated with the relationship between connection strength and topological network features. Our study is among the first studies of intelligence investigating the brain network topological features during a working memory task. Furthermore, it is the first intelligence study investigating brain network assortativity characteristics. Finally, we have implemented a recently developed mixed modeling framework for multitask studies, which considers the variability among node-specific topological characteristics instead of using the mean value of the topological network features. Our findings lend support to the idea that intelligence is associated with global efficiency, which helps with a more efficient flow of information between brain regions. Our results showed a higher positive association between global efficiency and connection strength for the higher intelligent group during the working memory task relative to the resting state. The stronger connection between the nodes with high global efficiency might act as superhighways for a more efficient flow of information. We also observed an increase in the negative association between assortativity measures and intelligence. The assortativity is associated with local information flow and the network's resilience. The decrease in the strength of connections of the nodes with less assortativity might lead to higher local information flow, which helps individuals with higher intelligence scores have a more circuit-specific information flow during working memory compared to the resting state. Taken together, we hypothesize that compared to the resting state, the brain's working memory network forms a network that, for higher performance, requires higher global

information flow through its superhighways with higher specific circuit information flow. Although the exact neurobiological implications of our results are speculative at this point, our results provide evidence for the significant association of intelligence with hallmark properties of brain networks during working memory. One limitation of our study was the short length of the working memory time series. We performed a separate analysis with the resting state being trimmed the same way as working memory data. Although the findings were qualitatively the same, there was not complete overlap between the results. The main concern would be that for the WM data we may have elevated false negative results. Thus, extra caution should be used when interpreting the analyses that did not find a significant association. Future studies can investigate the consistency of our findings using a different database with long working memory scans. Furthermore, future studies might focus on studying the subnetworks of the brain during a working memory task. Finally, these network properties might change over time, which static network analysis cannot capture. Future studies may focus on dynamic brain connectivity during working memory task as compared to resting state.

Supplementary Material

Refer to Web version on PubMed Central for supplementary material.

Acknowledgements

Data availability

The authors do not have permission to share data.

References

Alloway T, Alloway R, 2009. The efficacy of working memory training in improving crystallized intelligence. Nature Precedings 1, 1.

Anderson EL, Howe LD, Wade KH, Ben-Shlomo Y, Hill WD, Deary IJ, et al. , 2020. Education, intelligence and Alzheimer's disease: evidence from a multivariable two-sample Mendelian randomization study. Int. J. Epidemiol 49 (4), 1163–1172. [PubMed: 32003800]

Assem M, Blank IA, Mineroff Z, Ademo lu A, Fedorenko E, 2020. Activity in the fronto-parietal multiple-demand network is robustly associated with individual differences in working memory and fluid intelligence. Cortex 131, 1–16. [PubMed: 32777623]

Bahrami M, Laurienti PJ, Simpson SL, 2019. A MATLAB toolbox for multivariate analysis of brain networks. Hum. Brain Mapp 40 (1), 175–186. [PubMed: 30256496]

Barbey AK, 2018. Network neuroscience theory of human intelligence. Trends Cognit. Sci 22 (1), 8–20. [PubMed: 29167088]

Barch DM, Burgess GC, Harms MP, Petersen SE, Schlaggar BL, Corbetta M, et al. , 2013a. Function in the human connectome: task-fMRI and individual differences in behavior. Neuroimage 80, 169–189. [PubMed: 23684877]

Barch DM, Burgess GC, Harms MP, Petersen SE, Schlaggar BL, Corbetta M, et al. , 2013b. Function in the human connectome: task-fMRI and individual differences in behavior. Neuroimage 80, 169–189. [PubMed: 23684877]

Bassett DS, Bullmore E, 2006. Small-world brain networks. Neuroscientist 12 (6), 512–523. [PubMed: 17079517]

Bassett DS, Sporns O, 2017. Network neuroscience. Nat. Neurosci 20 (3), 353–364. [PubMed: 28230844]

Basten U, Stelzel C, Fiebach CJ, 2013. Intelligence is differentially related to neural effort in the task-positive and the task-negative brain network. Intelligence 41 (5), 517–528.

Cattell RB, 1987. Intelligence: its Structure, Growth and Action. Elsevier.

Cohen JR, D'Esposito M, 2016. The segregation and integration of distinct brain networks and their relationship to cognition. J. Neurosci 36 (48), 12083–12094. [PubMed: 27903719]

Cole MW, Yarkoni T, Repovs G, Anticevic A, Braver TS, 2012. Global connectivity of prefrontal cortex predicts cognitive control and intelligence. J. Neurosci 32 (26), 8988–8999. [PubMed: 22745498]

Colom R, Rebollo I, Palacios A, Juan-Espinosa M, Kyllonen PC, 2004. Working memory is (almost) perfectly predicted by g. Intelligence 32 (3), 277–296.

Cowan N, 2014. Working memory underpins cognitive development, learning, and education. Educ. Psychol. Rev 26 (2), 197–223. [PubMed: 25346585]

Crespi BJ, 2016. Autism as a disorder of high intelligence. Front. Neurosci 10, 300. [PubMed: 27445671]

Dizaji AS, Khodaei MR, Soltanian-Zadeh H, 2019. Resting-state fMRI Signals of Intelligent People Wander in a Larger Space, p. 529362 bioRxiv.

Duncan J, Owen AM, 2000. Common regions of the human frontal lobe recruited by diverse cognitive demands. Trends Neurosci. 23 (10), 475–483. [PubMed: 11006464]

Duncan J, Seitz RJ, Kolodny J, Bor D, Herzog H, Ahmed A, et al. , 2000. A neural basis for general intelligence. Science 289 (5478), 457–460. [PubMed: 10903207]

Finn ES, Shen X, Scheinost D, Rosenberg MD, Huang J, Chun MM, et al. , 2015. Functional connectome fingerprinting: identifying individuals using patterns of brain connectivity. Nat. Neurosci 18 (11), 1664–1671. [PubMed: 26457551]

Fischer FU, Wolf D, Scheurich A, Fellgiebel A, 2014. Association of structural global brain network properties with intelligence in normal aging. PLoS One 9 (1), e86258. [PubMed: 24465994]

Glasser MF, Sotiropoulos SN, Wilson JA, Coalson TS, Fischl B, Andersson JL, et al. , 2013. The minimal preprocessing pipelines for the Human Connectome Project. Neuroimage 80, 105–124. [PubMed: 23668970]

Haier RJ, Siegel BV, Nuechterlein KH, Hazlett E, Wu JC, Paek J, et al. , 1988. Cortical glucose metabolic rate correlates of abstract reasoning and attention studied with positron emission tomography. Intelligence 12 (2), 199–217.

Heaton RK, Akshoomoff N, Tulsky D, Mungas D, Weintraub S, Dikmen S, et al. , 2014. Reliability and validity of composite scores from the NIH Toolbox Cognition Battery in adults. J. Int. Neuropsychol. Soc. : JINS 20 (6), 588–598. [PubMed: 24960398]

Hilger K, Ekman M, Fiebach CJ, Basten U, 2017a. Intelligence is associated with the modular structure of intrinsic brain networks. Sci. Rep 7 (1), 16088. [PubMed: 29167455]

Hilger K, Ekman M, Fiebach CJ, Basten U, 2017b. Efficient hubs in the intelligent brain: nodal efficiency of hub regions in the salience network is associated with general intelligence. Intelligence 60, 10–25.

Hilger K, Fukushima M, Sporns O, Fiebach CJ, 2020. Temporal stability of functional brain modules associated with human intelligence. Hum. Brain Mapp 41 (2), 362–372. [PubMed: 31587450]

Joyce KE, Laurienti PJ, Burdette JH, Hayasaka S, 2010. A new measure of centrality for brain networks. PLoS One 5 (8), e12200. [PubMed: 20808943]

Jung RE, Haier RJ, 2007. The Parieto-Frontal Integration Theory (P-FIT) of intelligence: converging neuroimaging evidence. Behav. Brain Sci 30 (2), 135–154.; discussion 54–87. [PubMed: 17655784]

Kajantie E, Räikkönen K, Henriksson M, Leskinen JT, Forsén T, Heinonen K, et al. , 2012. Stroke is predicted by low visuospatial in relation to other intellectual abilities and coronary heart disease by low general intelligence. PLoS One 7 (11), e46841. [PubMed: 23144789]

Kanazawa S, 2013. Childhood intelligence and adult obesity. Obesity 21 (3), 434–440. [PubMed: 23404798]

Kanazawa S, 2014. General intelligence, disease heritability, and health: a preliminary test. Pers. Indiv. Differ 71, 83–85.

Kane MJ, Hambrick DZ, Conway ARA, 2005. Working memory capacity and fluid intelligence are strongly related constructs: comment on Ackerman, Beier, and Boyle (2005). Psychol. Bull 131 (1), 66–71. [PubMed: 15631552]

Kruschwitz JD, Waller L, Daedelow LS, Walter H, Veer IM, 2018. General, crystallized and fluid intelligence are not associated with functional global network efficiency: a replication study with the human connectome project 1200 data set. Neuroimage 171, 323–331. [PubMed: 29339311]

Laidra K, Pullmann H, Allik J, 2007. Personality and intelligence as predictors of academic achievement: a cross-sectional study from elementary to secondary school. Pers. Indiv. Differ 42 (3), 441–451.

Langer N, Pedroni A, Gianotti LR, Hänggi J, Knoch D, Jäncke L, 2012. Functional brain network efficiency predicts intelligence. Hum. Brain Mapp 33 (6), 1393–1406. [PubMed: 21557387]

Li Y, Liu Y, Li J, Qin W, Li K, Yu C, et al. , 2009. Brain anatomical network and intelligence. PLoS Comput. Biol 5 (5), e1000395. [PubMed: 19492086]

Longinetti E, Mariosa D, Larsson H, Almqvist C, Lichtenstein P, Ye W, et al. , 2017. Physical and cognitive fitness in young adulthood and risk of amyotrophic lateral sclerosis at an early age. Eur. J. Neurol 24 (1), 137–142. [PubMed: 28000353]

Malykh S, 2017. The role of personality traits and intelligence in academic achievement of Russian high school students. Procedia. Soc. Behav. Sci 237, 1304–1309.

Neubauer AC, Fink A, 2009. Intelligence and neural efficiency. Neurosci. Biobehav. Rev 33 (7), 1004–1023. [PubMed: 19580915]

Newman ME, 2002. Assortative mixing in networks. Phys. Rev. Lett 89 (20), 208701.

Newman MEJ, 2006. Modularity and community structure in networks. Proc. Natl. Acad. Sci. USA 103 (23), 8577–8582. [PubMed: 16723398]

Pamplona GS, Santos Neto GS, Rosset SR, Rogers BP, Salmon CE, 2015. Analyzing the association between functional connectivity of the brain and intellectual performance. Front. Hum. Neurosci 9, 61. [PubMed: 25713528]

Pruim RHR, Mennes M, van Rooij D, Llera A, Buitelaar JK, Beckmann CF, 2015. ICA-AROMA: a robust ICA-based strategy for removing motion artifacts from fMRI data. Neuroimage 112, 267–277. [PubMed: 25770991]

Santarnecchi E, Rossi S, Rossi A, 2015. The smarter, the stronger: intelligence level correlates with brain resilience to systematic insults. Cortex 64, 293–309. [PubMed: 25569764]

Santarnecchi E, Emmendorfer A, Tadayon S, Rossi S, Rossi A, Pascual-Leone A, 2017. Network connectivity correlates of variability in fluid intelligence performance. Intelligence 65, 35–47.

Satary Dizaji A, Vieira BH, Khodaei MR, Ashrafi M, Parham E, Hosseinzadeh GA, et al. , 2021. Linking brain biology to intellectual endowment: a review on the associations of human intelligence with neuroimaging data. Basic Clin. Neurosci 12 (1), 1–28. [PubMed: 33995924]

Shen X, Tokoglu F, Papademetris X, Constable RT, 2013. Groupwise whole-brain parcellation from resting-state fMRI data for network node identification. Neuroimage 82, 403–415. [PubMed: 23747961]

Simpson SL, Laurienti PJ, 2015. A two-part mixed-effects modeling framework for analyzing whole-brain network data. Neuroimage 113, 310–319. [PubMed: 25796135]

Simpson SL, Bahrami M, Laurienti PJ, 2019. A mixed-modeling framework for analyzing multitask whole-brain network data. Netw Neurosci 3 (2), 307–324. [PubMed: 30793084]

Tang CY, Eaves EL, Ng JC, Carpenter DM, Mai X, Schroeder DH, et al. , 2010. Brain networks for working memory and factors of intelligence assessed in males and females with fMRI and DTI. Intelligence 38 (3), 293–303.

van den Heuvel MP, Stam CJ, Kahn RS, Hulshoff Pol HE, 2009. Efficiency of functional brain networks and intellectual performance. J. Neurosci 29 (23), 7619–7624. [PubMed: 19515930]

Van Essen DC, Smith SM, Barch DM, Behrens TEJ, Yacoub E, Ugurbil K, et al. , 2013. The Wu-minn human connectome project: an overview. Neuroimage 80, 62–79. [PubMed: 23684880]

Waiter GD, Deary IJ, Staff RT, Murray AD, Fox HC, Starr JM, et al. , 2009. Exploring possible neural mechanisms of intelligence differences using processing speed and working memory tasks: an fMRI study. Intelligence 37 (2), 199–206.

Yeo RA, Arden R, Jung RE, 2011. Alzheimer's disease and intelligence. Curr. Alzheimer Res 8 (4), 345–353. [PubMed: 21222590]

Yeo RA, Ryman SG, van den Heuvel MP, de Reus MA, Jung RE, Pommy J, et al. , 2016. Graph metrics of structural brain networks in individuals with schizophrenia and healthy controls: group differences, relationships with intelligence, and genetics. J. Int. Neuropsychol. Soc 22 (2), 240–249. [PubMed: 26888620]

Yoo K, Rosenberg MD, Noble S, Scheinost D, Constable RT, Chun MM, 2019. Multivariate approaches improve the reliability and validity of functional connectivity and prediction of individual behaviors. Neuroimage 197, 212–223. [PubMed: 31039408]

Zalesky A, Fornito A, Seal ML, Cocchi L, Westin C-F, Bullmore ET, et al. , 2011. Disrupted axonal fiber connectivity in schizophrenia. Biol. Psychiatr 69 (1), 80–89.
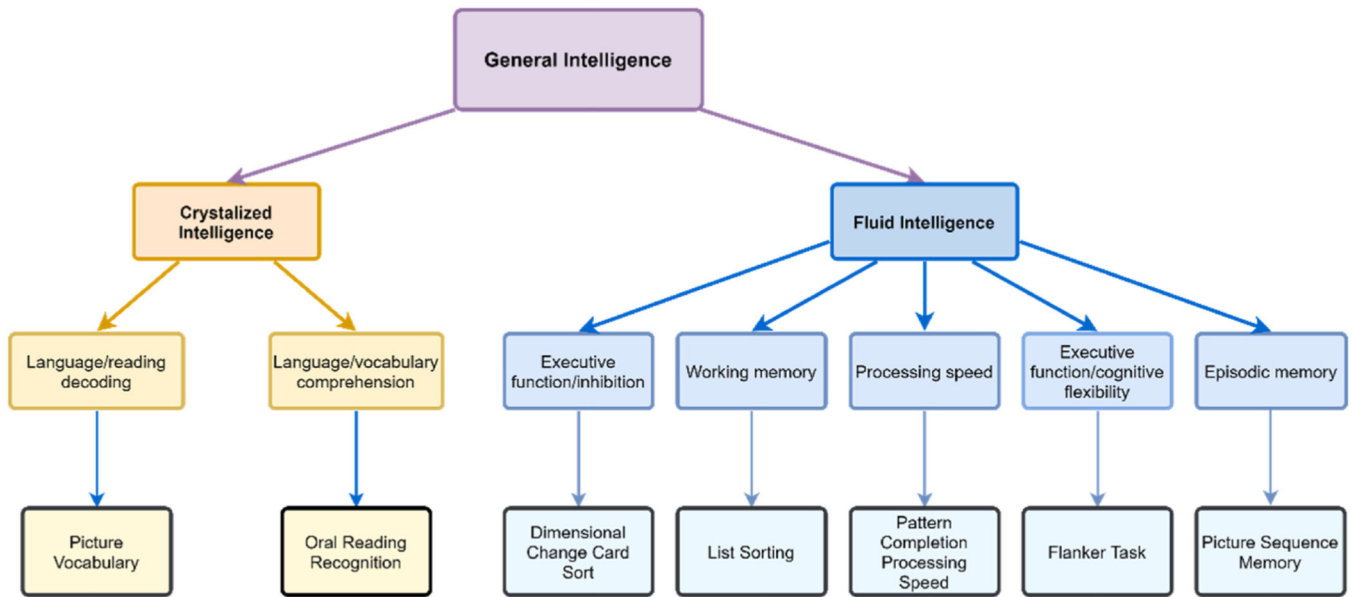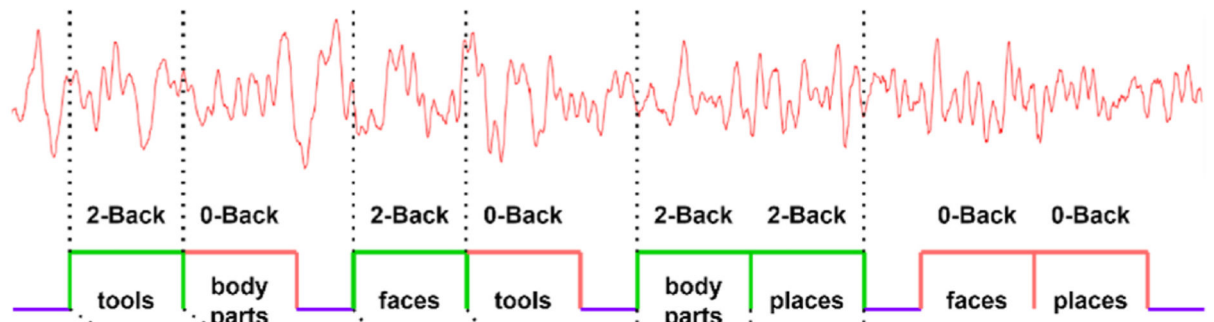
Fig. 1.
The NIH toolbox cognitive tests and their corresponding cognitive assessment. The first and the second row of the diagram show the composite scores. The third and fourth rows show the assessed cognitive abilities and the tests used respectively.
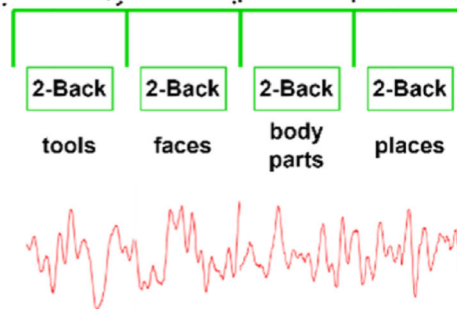
N-back Task Paradigm and Signal

Fig. 2.
Extraction and concatenation of 2-back working memory task signal. Top: the whole n-back task signal and paradigm which includes 2 back, 0 back and resting state. Bottom: 2 back task paradigm and time series.

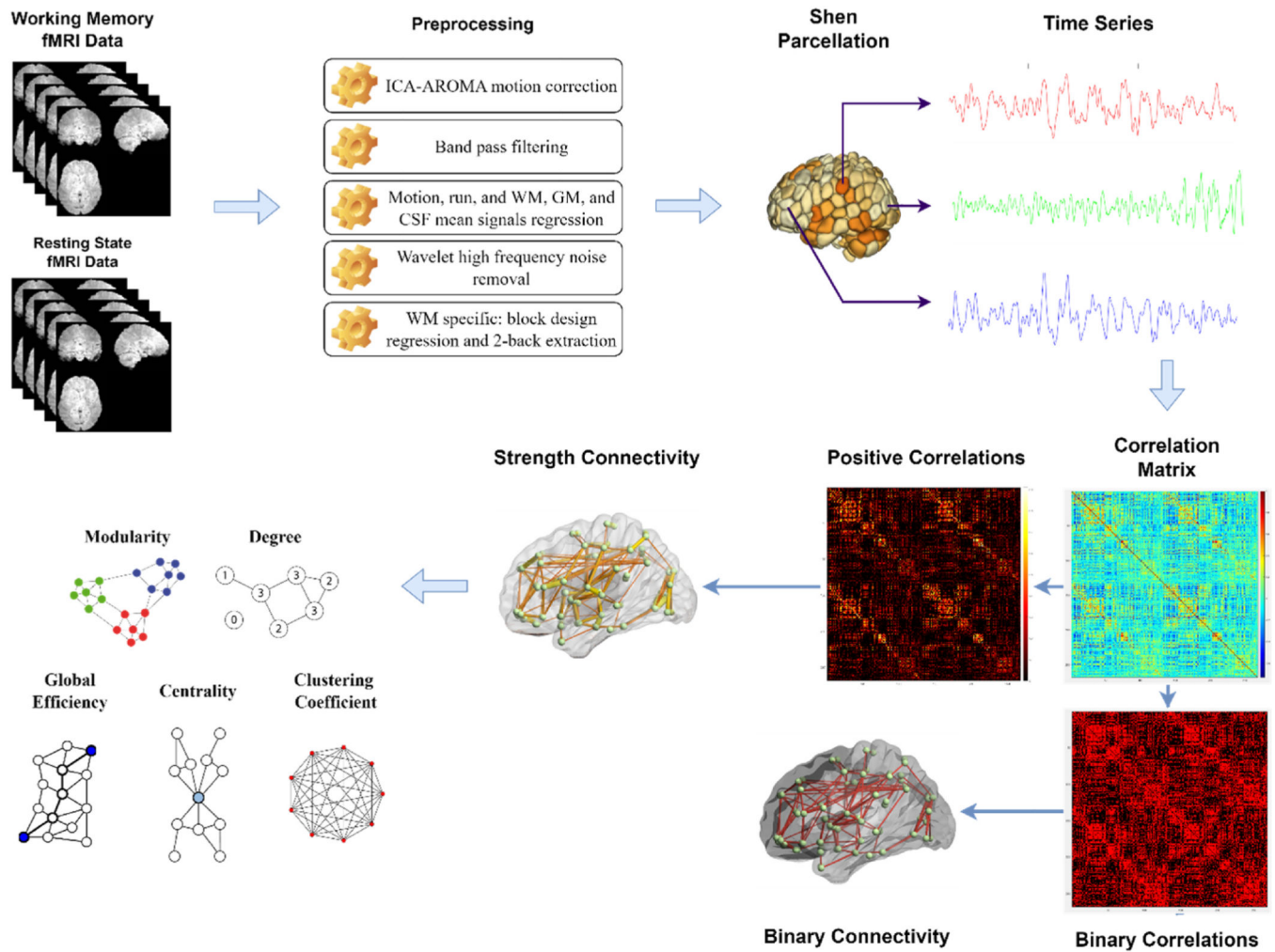**Fig. 3.**

The processing pipeline of the fMRI resting state and working memory data, including preprocessing, brain parcellation and time-series extraction, connectivity matrices estimation, and extraction of the five systemic network properties.
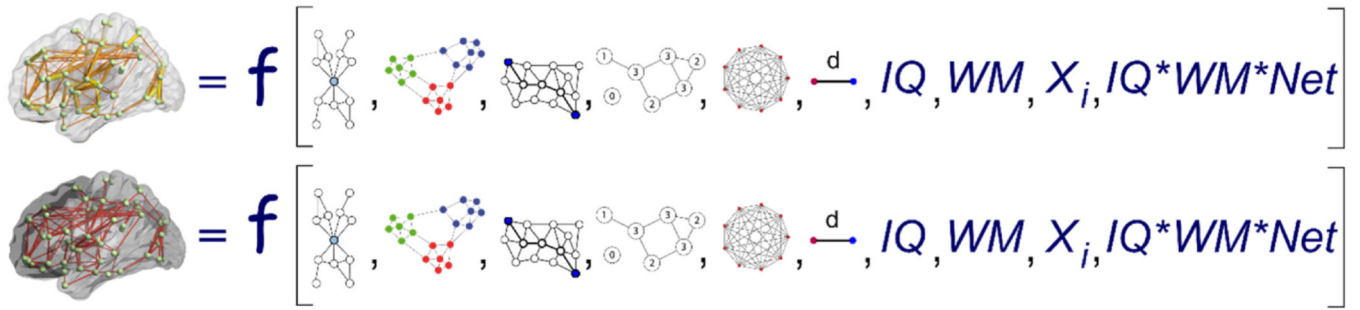
Fig. 4.
Two-part mixed modeling framework for strength and binary networks setup for investigation of intelligence during a working memory task and resting state. Top: Strength model, bottom: binary model. Each model includes five network measures, two distance measures (d), an intelligence group regressor as the covariate of interest (IQ), the task data indicator (WM), biological regressors (X_i), and the interactions of interest (IQ * WM * Net).

Edge characteristics

$$[Deg(i) - Deg(j)], [avg(Eglob(i), Eglob(j))], [avg(L_i, L_j)], [avg(C_i, C_j)], d, \ldots$$

Q, Task, COI, CON, INT

$= f$
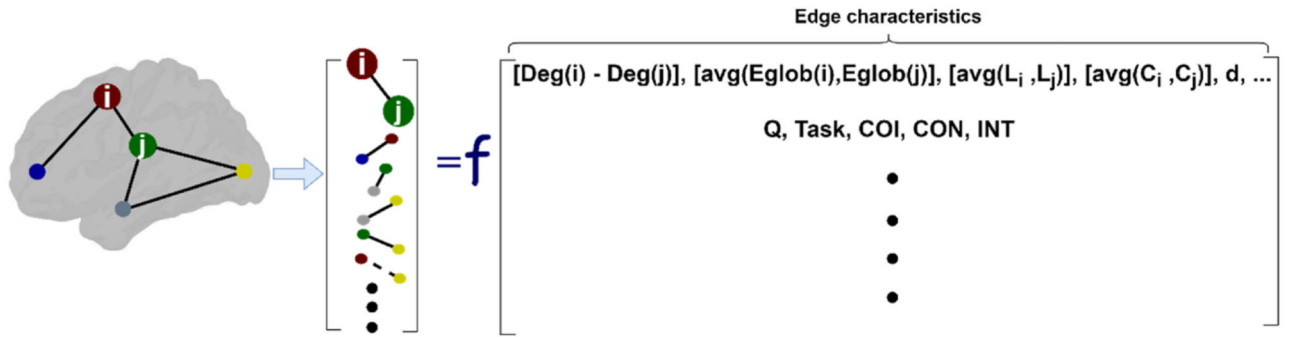
TOPOLOGICAL NETWORK MEASURE	MATHEMATIC FORMULA	NODE I	NODE J	EDGE (I,J) MEASURE	EDGE (I,J) VALUE
DEGREE	Number of connected nodes (K_i)	2	3	Deg(i) - Deg(j)	$1\,2 - 3\,1$
GLOBAL EFFICIENCY	$E_{glob} = \dfrac{1}{N-1} \sum_{j \neq i \in G} \dfrac{1}{d_{ij}}$			Avg (e_i, e_j)	$\dfrac{\frac{3}{4} + \frac{7}{8}}{2}$
LEVERAGE CENTRALITY	$L(v) = \dfrac{1}{K(v)} \sum_{v_i \in N_v} \dfrac{K(v) - K(v_i)}{K(v) + K(v_i)}$			Avg (L_i, L_j)	$\dfrac{\frac{1}{15} + \frac{2}{5}}{2}$
CLUSTERING COEFFICIENT	$C_i = \dfrac{2n_i}{K_i(K_i - 1)}$			Avg (C_i, C_j)	$\dfrac{0 + \frac{1}{3}}{2}$
MODULARITY	$Q = \dfrac{1}{(2m)} \sum_{ij} \left[A_{ij} - \dfrac{k_i k_j}{(2m)} \right] \dfrac{s_i s_j + 1}{2}$			Q of the network	0.24
DISTANCE	Euclidian distance between brain region pairs			d	5 cm

Fig. 5.

Top. Hypothetical example of elements of each row of the mixed model framework. On the left of the equations, strength (or existence) of edge and on the right of the equation, degree difference (deg), average global efficiency (e), average leverage centrality (L), average clustering coefficient (C), modularity (Q), nodes distance (d), task identifier (Task), covariate of interest (COI), biological confounds (CON) and interactions (INT) exist. **Bottom**. A schematic of how each edge measure will be computed for the mixed model framework. First, the topological network feature of nodes i and j is extracted separately using the presented formulas. Next, the average (in the case of degree, the difference) of the two nodes of each edge is computed. For modularity, the whole network modularity is used for all edges. Finally, node distances were estimated by calculating the Euclidean distance between each pair. The last column shows estimation of the edge features for the example cartoon brain. (k: node degree, e:global efficiency, N: number of nodes, d: shortest

distance, L:leverage centrality, C:clustering coefficient, n: number of connected neighbors, Q: modularity, m: number of edges, A: adjacency matrix).
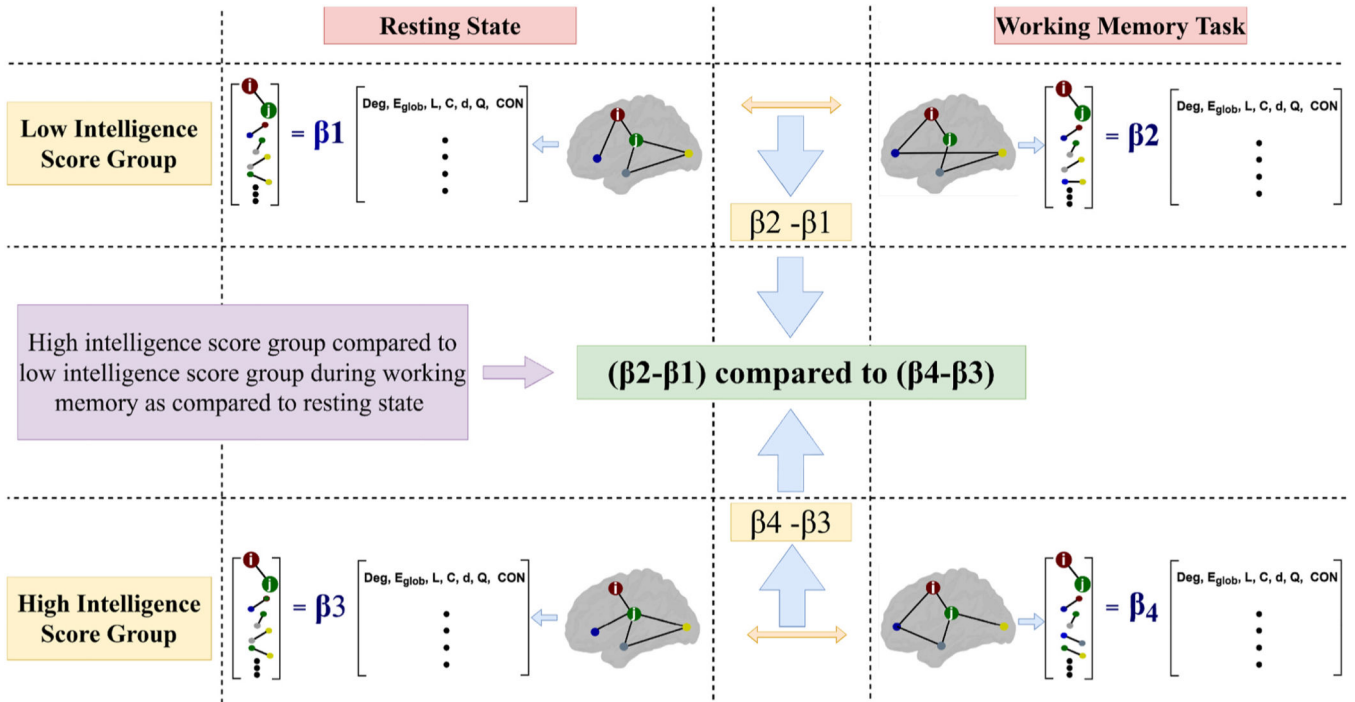
Fig. 6.

The breakdown of the parameters of interest in the multi-task mixed modeling framework. The main parameter of interest is the difference in the association of edge topological network features and connection strength (or connection probability) between the two groups (high and low intelligence scores) when their working memory is compared to the resting state.

a. Global Efficiency
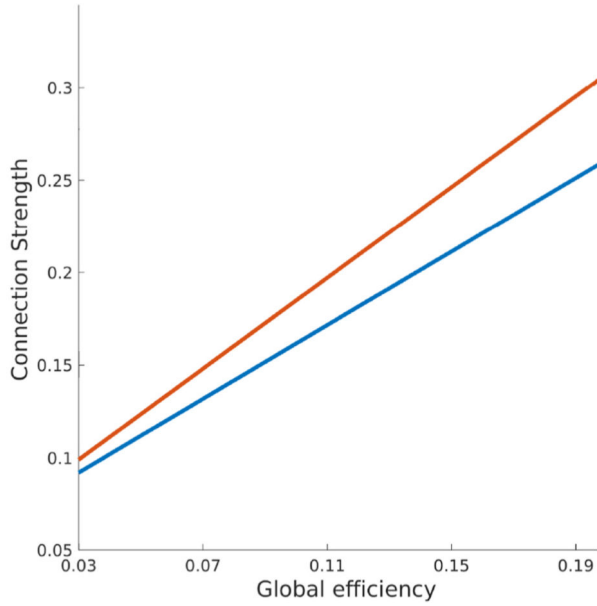
b. Degree Difference

c. Leverage Centrality

low G-Score group
high G-Score group
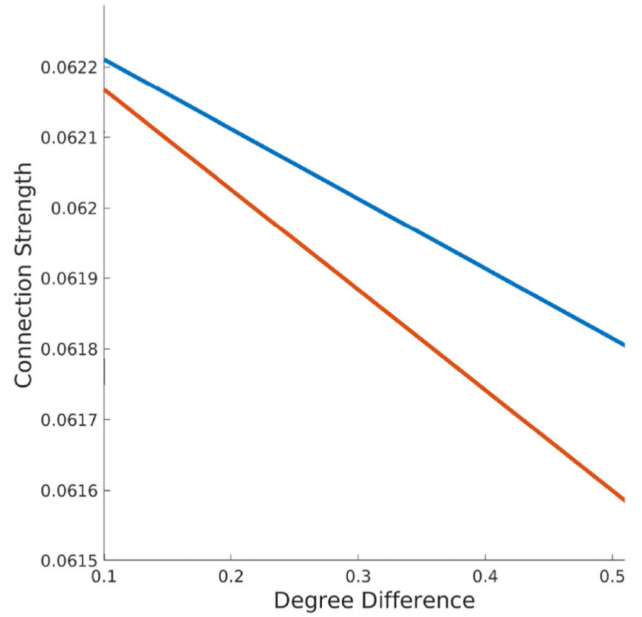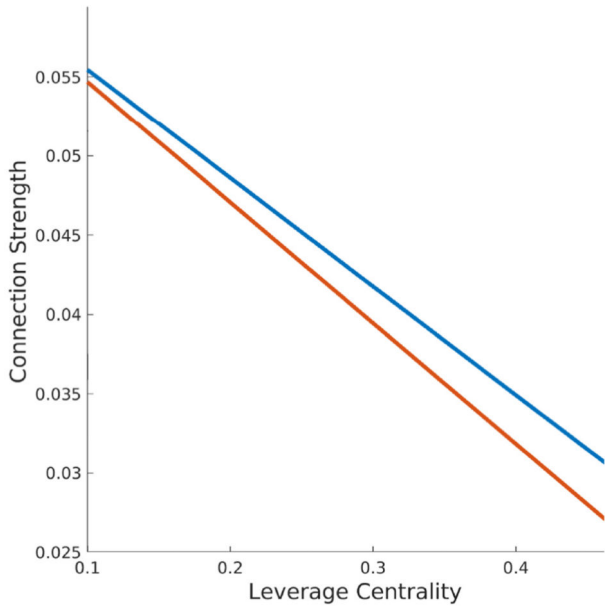
Fig. 7.
The association between connection strength and topological network features for high and low general intelligence groups during working memory task when it is compared to resting state. a. Intelligence has increased the association between connection strength and global efficiency. b, c. Intelligence increased the negative association between connection strength and centrality measures, including leverage centrality and degree difference.

Table 1

Demographic information and cognitive score of the sample of HCP data used in this study.

Variable	Mean ± standard deviation	count
Number of subjects		379
Gender (male/female)		174/205
Age	28.71 ± 3.70	
Handedness (− 100 < x < 100)	65.98 ± 43.29	
BMI	26.19 ± 5.01	
Income (1/2/3/4/5/6/7/8)	5.03 ± 2.20	
Education level (1/2/3)		61/260/58
Race (1/2/3/4/5/6)		1/32/46/282/11/7
Ethnicity		39/332/8
DSM4 alcohol abuse (0/1)		314/65
DSM4 alcohol dependence (0/1)		355/24
Smoke Status (0/1)		320/59
Dimensional change card sort	115.22 ± 9.86	
List sorting	111.28 ± 11.19	
Pattern completion processing speed	116.21 ± 15.14	
Flanker task	111.56 ± 9.82	
Picture sequence memory	113.06 ± 13.62	
Picture vocabulary	117.21 ± 9.26	
Oral reading recognition	117.16 ± 10.62	
Fluid cognition composite score	115.94 ± 11.02	
Crystalized cognition composite score	118.12 ± 9.65	
Total cognition composite score (general intelligence)	122.94 ± 14.24	

Table 2

Results of running the two-part mixed modeling framework on HCP data with high and low scoring general intelligence groups as the covariate of interest. The strength model shows a significant effect of the general intelligence composite score on describing the difference (from resting state) in the relationship between network measures and connectivity strength during a working memory task. More specifically, general intelligence affects the relationship between global efficiency, degree difference, and leverage centrality and the strength of connections. No significant relationship was observed for the binary model.

Model used	Parameter	Estimate	t-value	P-value	Adaptive FDR
Strength model	$\beta_{s, WM \times IQ \times Eglob\_avg}$	**0.2325**	**2.43**	**0.0153**	**0.0236**
	$\beta_{s, WM \times IQ \times deg\_diff}$	**−0.00043**	**−2.36**	**0.018**	**0.0267**
	$\beta_{s, WM \times IQ \times lev\_avg}$	**−0.00771**	**−2.26**	**0.0241**	**0.0328**
	$\beta_{s, WM \times IQ \times mod}$	0.2287	0.93	0.3533	0.3533
	$\beta_{s, WM \times IQ \times clust\_avg}$	−0.103	−1.66	0.0976	0.108
Binary model	$\beta_{r, WM \times IQ \times Eglob\_avg}$	− 0.1355	−0.11	0.914	0.914
	$\beta_{r, WM \times IQ \times deg\_diff}$	−0.00053	−0.29	0.7748	0.795
	$\beta_{r, WM \times IQ \times lev\_avg}$	−0.01272	−0.28	0.7788	0.795
	$\beta_{r, WM \times IQ \times mod}$	−1.1772	−1.22	0.2215	0.4309
	$\beta_{r, WM \times IQ \times clust\_avg}$	0.768	0.71	0.48	0.5881

Table 3

Results of running the two-part mixed modeling framework on HCP data with high and low scoring fluid intelligence groups as the covariate of interest. The strength model shows a significant effect of the fluid intelligence composite score on describing the relationship between degree difference and connectivity strength during a working memory task as compared to resting state. No significant relationship was observed for the binary model.

Model used	Parameter	Estimate	t-value	P-value	Adaptive FDR
Strength model	$\beta_{s, WM \times IQ \times Eglob\_avg}$	0.07276	0.76	0.4502	0.4502
	$\beta_{s, WM \times IQ \times deg\_diff}$	**−0.00038**	**−2.12**	**0.0339**	**0.057**
	$\beta_{s, WM \times IQ \times lev\_avg}$	−0.00419	−1.22	0.2215	0.2562
	$\beta_{s, WM \times IQ \times mod}$	−0.02579	−0.1	0.9169	0.9169
	$\beta_{s, WM \times IQ \times clust\_avg}$	−0.06816	−1.09	0.2739	0.2896
Binary model	$\beta_{r, WM \times IQ \times Eglob\_avg}$	0.2286	0.18	0.8553	0.8553
	$\beta_{r, WM \times IQ \times deg\_diff}$	−0.00201	−1.1	0.2728	0.4364
	$\beta_{r, WM \times IQ \times lev\_avg}$	−0.01071	−0.24	0.8128	0.8128
	$\beta_{r, WM \times IQ \times mod}$	0.1945	0.2	0.8405	0.8405
	$\beta_{r, WM \times IQ \times clust\_avg}$	0.3272	0.3	0.7634	0.7634

Table 4

Results of running the two-part mixed modeling framework on HCP data with high and low scoring crystallized intelligence groups as the covariate of interest. The strength model shows a significant effect of the crystallized intelligence composite score on describing the relationship between global efficiency and connectivity strength during a working memory task as compared to resting state. No significant relationship was observed for the binary model.

Model used	Parameter	Estimate	t-value	P-value	Adaptive FDR
Strength model	$\beta_{s,\,WM \times IQ \times Eglob\_avg}$	**0.2377**	**2.48**	**0.013**	**0.0269**
	$\beta_{s,\,WM \times IQ \times deg\_diff}$	−0.00021	−1.14	0.2532	0.2686
	$\beta_{s,\,WM \times IQ \times lev\_avg}$	−0.00643	−1.88	0.0603	0.0879
	$\beta_{s,\,WM \times IQ \times mod}$	−0.2605	−1.05	0.2915	0.2939
	$\beta_{s,\,WM \times IQ \times clust\_avg}$	−0.02121	−0.34	0.734	0.734
Binary model	$\beta_{r,\,WM \times IQ \times Eglob\_avg}$	−0.621	−0.5	0.62	0.6561
	$\beta_{r,\,WM \times IQ \times deg\_diff}$	0.002085	1.14	0.2555	0.4054
	$\beta_{r,\,WM \times IQ \times lev\_avg}$	0.03097	0.69	0.4931	0.5447
	$\beta_{r,\,WM \times IQ \times mod}$	−0.4125	−0.43	0.6704	0.6704
	$\beta_{r,\,WM \times IQ \times clust\_avg}$	−0.285	−0.26	0.7934	0.7934